Microwave-Assisted Synthesis of Manganese Oxide Octahedral Molecular Sieve (OMS-2) Nanomaterials under Continuous Flow Conditions

Naftali N. Opembe,[†] Cecil K. King'ondu,[†] Anais E. Espinal,[‡] Chun-Hu Chen,[†] Edward K. Nyutu,[†] Vincent M. Crisostomo,[†] and Steven L. Suib*,[†,‡]

Department of Chemistry, University of Connecticut, Storrs, Connecticut 06269-3060, and Institute of Materials Science, University of Connecticut, Storrs, Connecticut 06269-3136

Received: May 21, 2010; Revised Manuscript Received: July 26, 2010

A continuous flow microwave method has been developed for the synthesis of cryptomelane-type K-OMS-2 nanomaterials in a mixed aqueous−organic solvent system. The system is ideal for multikilogram synthesis of K-OMS-2 nanomaterials. The synthesized nanomaterials have crystallite sizes of about 1.8 nm with a surface area of 213 m^2/g. X-ray diffraction (XRD), electron microscopy (SEM and TEM), thermogravimetric analysis (TGA), differential scanning calorimetry (DSC), infrared spectroscopy (FTIR), nitrogen sorption experiments, and potentiometric titrations have been used to characterize the nanomaterials. Kinetically, an increase in power has a direct relation to increase in temperature, and this has an effect on reaction rate. The synthesized materials show excellent results in the oxidation of 2,3,6-trimethylphenol.

Introduction

Microwave-assisted chemistry has matured from a curiosity to an established synthesis technology that finds use in both academia and industry. Microwave-assisted synthesis has led to dramatic lowering of reaction times,[1−3] higher product yields,[4,5] and even much purer products.[5] The major heating mechanisms involved in microwave heating are dipolar polarization or ionic conduction[6,7] due to the interactions of dielectric materials (both liquids and solids) with the microwave electromagnetic field. The ability of a material or a reaction medium to convert electromagnetic energy into heat at a given frequency and temperature is related to the loss tangent ($\tan \delta$), itself a ratio of the material's dielectric constant (ε'') and dielectric loss factor (ε').[8−10] A material with a high $\tan \delta$ couples well with a microwave field, consequently leading to rapid heating (superheating).

However, one drawback of microwave chemistry is the difficulty associated with reaction scale-up. The problem emanates from establishing safe and reliable processes where penetration depths, control of the temperature, and reactor design are crucial parameters. In a batch scale-up, microwaves lack penetration power, thereby heating only the solution at the periphery of the reaction vessel.[10−13] Therefore, the bulk of the reaction mixture is heated through a conventional heat transfer process and not by microwaves. This renders microwave chemistry ineffective in performing multikilogram syntheses on a batch mode. The solution to this drawback lays in the use of a continuous flow process[14] whereby reactant flow rates and microwave residence times dictate the scale of the synthesis. The need for big reaction vessels is replaced with tubular reactors with an inner diameter of a few millimeters and capable of producing multikilogram quantities of materials. Reactant streams are continuously pumped into the reactor while product streams continuously leave the reactor at the discharge end.
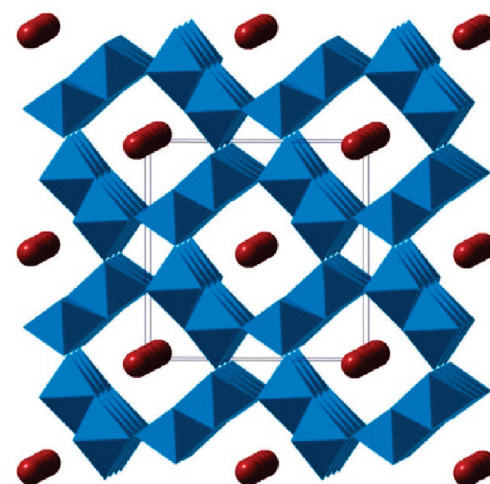

Figure 1. Crystal structure representation of K-OMS-2 with potassium (K+) counter cations shown as maroon spheres and MnO$_6$ octahedra shown as blue octahedra. The tetragonal unit cell ($a = b = 9.82$ Å, $c = 2.85$ Å) is also shown with blue lines.

Cryptomelane-type manganese oxide octahedral molecular sieves (OMS-2) belong to a group of manganese oxides having a 2×2 tunnel structure formed by edge and corner sharing of manganese oxide (MnO$_6$) octahedra, resulting in a one-dimensional (1-D) channel as illustrated in Figure 1.[15−18] Positive cations, for instance, potassium (and hence K-OMS-2), and water molecules occupy the tunnels. The tunnel cations can be partially or fully ion-exchanged with other ions. For instance, exchange with protons (H+) gives its acidic form, H-K-OMS-2. These materials have been used as catalysts in numerous studies, such as selective oxidation of alcohols,[17a] 9H-fluorene,[19] and cyclohexene,[20] epoxidation of styrene and other olefinic substrates,[21] synthesis of 2-aminodiphenylamine,[22] decomposition of dyestuffs,[23] oxidative dehydrogenation of ethane[24] among other reactions. Alternatively, they can be used as molecular sieves in separation processes[25] or in energy storage applications.[26] K-OMS-2 is mixed valent with manganese found in oxidation states of Mn^{2+}, Mn^{3+}, and Mn^{4+}.[33]

* To whom correspondence should be addressed. Phone: 860-486 2797. Fax: 860-486 2981. E-mail: steven.suib@uconn.edu.
† Department of Chemistry.
‡ Institute of Materials Science.

The synthesis of K-OMS-2 materials has been realized through different routes.[15,17,18] Systematic studies have been done to among others reduce the particle size to the nanometer range. Villegas et al.[15] successfully prepared nanosized crystalline K-OMS-2 fibers with crystallite sizes as low as 6 nm by reducing $KMnO_4$ with H_2O_2 in an acidic buffer medium in about 15 h, under conventional reflux. Recently, Nyutu et al.[27,28] reported a method for synthesizing K-OMS-2 in mixed aqueous and nonaqueous solvents by use of microwave reflux, obtaining K-OMS-2 nanomaterials with crystallite sizes as low as 4 nm. This method required about 10 min to start crystallizing the K-OMS-2 phase and about 90 min to fully crystallize the phase. Crisostomo[29] developed a continuous flow method for synthesizing CeO_2, $CoOOH$, and $FeOOH$ using microwave irradiation.

In this Article, we report forthwith a systematic study of the continuous flow synthesis of K-OMS-2 materials using microwave irradiation utilizing a process similar to the one developed by Crisostomo[29] and using a cosolvent system from Nyutu. This was accomplished by investigating the effect of important parameters such as microwave irradiation power, cosolvent amount (% DMSO), and reactant flow rates (and hence microwave residence times). By continuously flowing a reactant mixture through a microwave cavity and by a correct choice of power, DMSO amount, and flow rates, it was possible to establish optimal conditions that allowed the continuous mass production of pure nanofibrous K-OMS-2. This technique can be adopted for potential large scale industrial synthesis of this and other nanomaterials.

Experimental Methods

Materials. Potassium permanganate ($KMnO_4$), manganese sulfate monohydrate ($MnSO_4 \cdot H_2O$), 2,3,6-trimethylphenol (TMP), dimethyl sulfoxide (DMSO) (99.9%, Acros), acetonitrile (MeCN), and *tert*-butyl hydroperoxide (70% in water TBHP) were purchased from Sigma-Aldrich, while concentrated nitric acid (HNO_3) was obtained from Alfa Aesar. All reagents were used without any further purification.

Microwave Setup. Continuous flow syntheses were carried out in a *CEM Mars 5* multimode microwave (see Figure S1 of the Supporting Information for a pictorial). The microwave is equipped with one magnetron, a fixed frequency of 2.45 GHz, and a three-level power output of 300, 600, and 1200 W, where power at each level can be controlled within a 0–100% range. The system can use a temperature-sensing device (fiber-optic) for *in situ* measurements of temperature inside open or sealed reaction vessels and also contains an in-board pressure control system to monitor and control reaction pressures inside sealed reaction vessels. The apparatus has overall dimensions of 25″ × 20″ × 23 ″ (D × W × H). The microwave can be operated in any of the following five control modes: standard control, ramp to temperature, ramp to pressure, power/time control, and microvap. Temperature and pressure can be set and monitored in all except the power/time control mode where power and time are the only variables. The power/time control mode was used, since the reactor configuration does not allow for adaptation of temperature or pressure-monitoring devices. Inside the microwave cavity, a coiled tubular reactor made of Teflon and with dimensions of $\Phi_{inner} = 1/8″$, $\Phi_{outer} = 1/4″$, $\Phi_{coil} = 1\text{-}1/2″$, and $L = 72″$ was used. The coiled reactor was continuously fed with feedstock by use of a peristaltic pump connected to the coiled tubular reactor inlet and operated from outside the microwave. Only the coiled part of the reactor was directly irradiated with the microwaves (see Figure 2 for a schematic diagram). The peristaltic pump controlled the feed
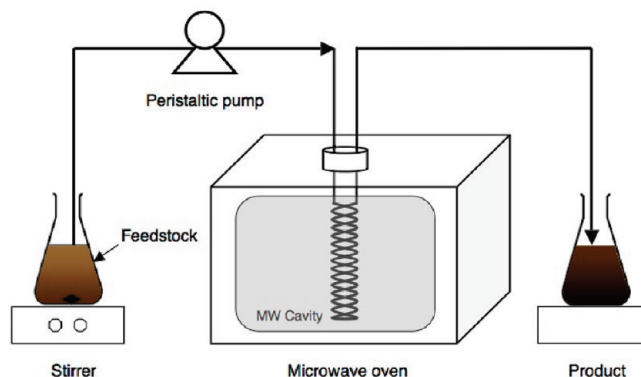

Figure 2. Schematic drawing of the continuous flow synthesis setup showing a coiled Teflon reactor inside the microwave cavity.

flow rates. All reactions were nominally run at atmospheric pressure, since both the feeding and sampling ends were open. Effects of feed flow rates, microwave residence times, and influence of microwave power on the synthesis were investigated.

Microwave Treatments. The microwave was run in the power/time mode with power being varied betwen 150, 300, 450, and 600 W by changing percentage power at 600 W by 25, 50, 75, and 100%, respectively. In the power/time mode, temperature can neither be controlled nor monitored.

Synthesis. K-OMS-2 syntheses have been done using different approaches. We chose a recently reported method,[27] which involves the use of microwave irradiation in aqueous and nonaqueous systems. The chosen method utilizes the symproportionation by Mn^{2+} and Mn^{7+} ions present in manganese sulfate and potassium permanganate, respectively. In a typical reaction, 42 mmol (6.65 g) of $KMnO_4$ was added to 100 mL of distilled–deionized water (DDW) to make mixture A. In another flask, 59 mmol (9.9 g) of $MnSO_4 \cdot H_2O$ was added to 33 mL of DDW to make mixture B. Both A and B were stirred separately until complete dissolution of the reagents. To B, 3.4 mL of concentrated HNO_3 was added and further stirred. Solution A was transferred to a dropping funnel and dropwise added to solution B under vigorous stirring. The resultant mixture (C) was further stirred at room temperature for a further 15 min before addition of different volumes of DMSO to make up various percentages (v/v).

For instance, to make 10% (v/v) DMSO in C, 15 mL of DMSO was added to C. DMSO-containing mixture C was kept stirring in a flask throughout the duration of the microwave treatment. Rubber tubing was connected to this flask and to a peristaltic pump and further connected to the inlet of a coiled reactor that was maintained in the microwave cavity. Reactants were continuously pumped through the coiled reactor in the microwave cavity at different flow rates, where they interacted with microwave irradiation for a given duration of time. Products were thereafter collected at the discharge end of the reactor into a collecting flask, washed with distilled–deionized water (DDW), centrifuged, and dried overnight at 120 °C in an oven.

As a starting point, the power was fixed at 300 W and DMSO at 10%. With these parameters fixed, we studied the effect of flow rates by varying the flow by 40 mL/min (MC-10-40 mL/min), 20 mL/min (MC-10-20 mL/min), 10 mL/min (MC-10-10 mL/min), and 5 mL/min (MC-1005 mL/min). Next, the power at 300 W and the flow rate at 10 mL/min were held constant and the amount of DMSO varied as follows: 0% (MC-0-10 mL/min), 5% (MC-5-10 mL/min), and 25% (MC-25-10 mL/min). These were compared to the 10% DMSO above, i.e., MC-10-10 mL/min. A similar study was done at a higher flow rate of

Synthesis of Manganese Oxide OMS-2 Nanomaterials

J. Phys. Chem. C, Vol. 114, No. 34, 2010 **14419**

20 mL/min, but the amount of DMSO was kept at 5% (MC-5-20 mL/min), 25% (MC-25-20 mL/min), and 50% (MC-50-20 mL/min), comparing the results to the MC-10-20 mL/min sample. Effects of the reactor configuration in the synthesis and varying the microwave power from 150 to 600 W were also studied. As for the reactor configuration study, the coiled tubular reactor was replaced with a noncoiled reactor of similar dimensions.

Characterization Methods. The powder X-ray diffraction studies were performed on a Scintag XDS-2000 diffractometer using Cu Kα ($\lambda = 0.15406$ nm) radiation and operating at a beam voltage of 45 kV and a current of 40 mA. Data were collected continuously in the 2θ range of 5−75° at a scan rate of 1.0 deg/min and the phase identified using a JCPDS database card number 29-1020. The XRD patterns of samples were collected on either a glass or an aluminum sample holder. The crystallite particle sizes of the prepared K-OMS-2 materials were determined by applying the Debye−Scherrer equation to the reflections at (310) and (211) of the XRD patterns with the integral widths corrected using a LaB_6 standard.

Morphology. The morphology of the products was studied by field emission scanning electron microscopy (FE-SEM) on a Zeiss DSM 982 Gemini instrument with a Schottky emitter at an accelerating voltage of 2 kV and a beam current of 1 mA. The carbon tape mount method was used where powder samples were dispersed in iso-propanol in a glass vial and ultrasonicated prior to being dispersed on Au−Pd-coated silicon glass chips previously mounted onto aluminum slabs with a two-sided carbon tape and dried by vacuum desiccation prior to SEM studies. TEM studies were carried out with a JEOL 2010 UHR FasTEM, operating at an accelerating voltage of 200 kV and equipped with an energy dispersive X-ray analysis (EDS) system. The samples were prepared by dispersing the powder material in 2-propanol. A drop of the dispersion was placed onto a wholly carbon-coated copper grid and allowed to dry.

Surface Area and Pore Size Distribution. This was performed using nitrogen sorption on a Micrometrics ASAP 2010 accelerated surface area system. Samples were degassed at 120 °C for 12 h prior to the adsorption−desorption experiments which were carried out at 77 K. The specific surface area of the material was determined with the Brunauer−Emmett−Teller (BET) method, while the pore size distribution was determined using the Barrett−Joyner−Halenda (BJH) method.

Thermal Stability and Potentiometric Titrations. Thermogravimetric analysis (TGA) and differential scanning calorimetry (DSC) were employed to study the thermal behavior of the samples. The TGA experiments were performed with a Hi-Res TA Instruments Model 2950, while differential scanning calorimetry (DSC) experiments were performed on a DSC Model Q20. In both experiments, temperature was increased at a ramp rate of 20°/min in a nitrogen atmosphere. Potentiometric titrations[15] were performed to determine the average oxidation state (AOS) of manganese in the synthesized materials.

Surface and Functional Group Studies. The surface and functional group properties of the prepared materials were studied by Fourier transform infrared (FTIR) spectroscopy, using a Nicolet Magna-IR Model 560 in the range 4000−400 cm^{-1} with a DTGS detector. K-OMS-2 powders were diluted in a ratio of 1:100 with KBr and then pressed into pellets at about 15000 psi.

Catalytic Applications. The synthesized K-OMS-2 materials were used in the oxidation of 2,3,6-trimethylphenol (TMP) using *tert*-butyl hydroperoxide as the oxidant. The heterogeneous liquid-phase oxidation reactions were performed batch-wise.

K-OMS-2 catalyst (50 mg) previously dried at 120 °C for 4 h was added to a 50 mL two-neck round-bottom flask containing 1 mmol of TMP in 10 mL of acetonitrile as a solvent and TBHP. The reaction mixture was stirred and refluxed in the oil-bath at 80 °C for 4 h, after which the product was filtered and analyzed.

The identification and quantitative analysis of the reaction products was performed using GC-MS. This was done using an HP 5890 Series II gas chromatograph equipped with an HP 5971 mass selective detector coupled with a TCD detector. Separation was carried out in a nonpolar column (HP-1).

Results

Continuous Formation of K-OMS-2 Nanomaterials. The symproportionation of Mn^{7+} and Mn^{2+} in the mixed aqueous−organic solvent system is responsible for the formation of the cryptomelate-type K-OMS-2. When $KMnO_4$ solution was added to the $MnSO_4 \cdot H_2O$ solution that contained nitric acid, the mixture turned light brown in color and changed to a darker brown shade with the addition of more $KMnO_4$ solution. This color did not change significantly upon addition of DMSO. The mixture was thin enough to allow for its flow in the coiled reactor. This precipitate was not analyzed, since XRD results of a similar precipitate[27] showed a poorly ordered K-OMS-2 phase. We chose 10% DMSO and a 300 W power level as the starting point for our study. The % DMSO choice was based on results from a previous report[27] which used a mixed aqueous and nonaqueous system in a batch process. It is reported therein that a 10% DMSO mixture produced a crystalline phase of K-OMS-2 after 90 min reaction time in the same microwave apparatus. In this study, a peristaltic pump controlled the flow rates. The mixture was continuously fed at 40, 20, 10, and 5 mL/min flow rates with corresponding residence times of less than a minute (∼50 s), 2 min, 4 min, and 8 min, respectively, and at a constant microwave power of 300 W. X-ray diffraction was used to confirm the crystal phase. At 40 mL/min, a poorly ordered manganese oxide phase was obtained, as shown in Figure 3 (MC-10-40 mL/min). At 20 mL/min, the phase was less poorly ordered (MC-10-20 mL/min) with peaks characteristic of K-OMS-2 (JCPDS 29-1020) evident, albeit with an impurity phase ($2\theta = 23°$). A slower rate of 10 mL/min led to a much purer and more crystalline phase of K-OMS-2. A similar pure phase was obtained at 5 mL/min.

We sought to study the effects of % volume of DMSO at different flow rates on the synthesis of K-OMS-2. Figure 4 shows the resultant XRD patterns. At 10 mL/min, when no DMSO is added to the synthesis mixture, transformation to the K-OMS-2 phase does not occur. Similar results are to be expected at 20 mL/min and higher rates. At 5% DMSO, evolution of broad K-OMS-2 peaks was observed, indicating the formation of small crystallites (see MC-5-10 mL/min and MC-5-20 mL/min in Figure 4). However, at this DMSO level, phase impurity was observed.

Similar peak broadening was also observed at the 10% DMSO level at both the 10 and 20 mL/min flow rates (see MC-10-10 mL/min and MC-10-20 mL/min), but the latter sample had an impurity phase that was absent from the former. Syntheses with 25% DMSO at both flow rates (see MC-25-10 mL/min and MC-25-20 mL/min) led to pure K-OMS-2. At 20 mL/min, both the 25 and 50% DMSO level samples showed consistently broader peaks with no impurities (see MC-25-20 mL/min and MC-50-20 mL/min). The Debye−Scherrer equation was applied to the (310) and (211) XRD reflections to estimate the crystallite sizes of the materials in Figure 4 with the exception of the materials that did not transform to K-OMS-2 or had pronounced impuri-
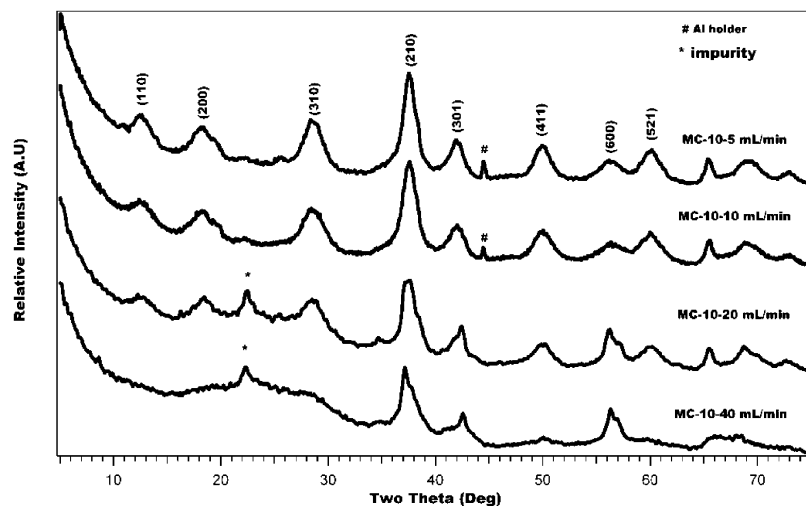
Figure 3. XRD patterns of K-OMS-2 showing the effect of reactant flow rates at constant microwave power (300 W) and constant volume of DMSO (10% v/v). The reactant flow rate was varied from 40 mL/min down to 5 mL/min.
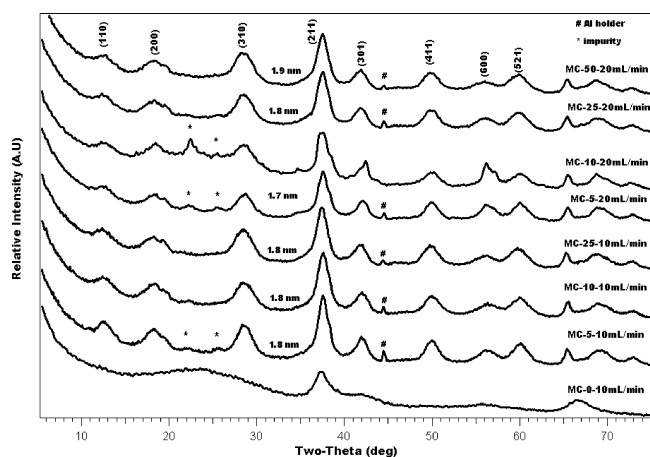

Figure 4. XRD patterns of K-OMS-2 prepared using different percentages of the cosolvent (DMSO) at two flow rates, 10 and 20 mL/min. The phases were matched to the Q-phase of cryptomelane (KMn$_8$O$_{16}$; JCPDS 29-1020).

ties. The calculated crystallite size results are part of Figure 4. All the materials synthesized at 300 W at either 10 or 20 mL/min and with different percentages of DMSO had almost similar crystallite sizes ranging between 1.6 and 1.8 nm.

We sought to find out what the exact temperatures at the various power levels used were, since in the power/time mode used we could not monitor this parameter. While in the power/time mode, we fixed the power at 300 W and carried out batch reactions on small volumes (10 mL) of the reaction mixture for time periods similar to retention times in the flow process while using a thermometer to measure the reaction temperature. We also studied the temperature at different power levels at a fixed residence time of 4 min. Figure S2 of the Supporting Information shows the XRD patterns as well as temperatures measured for these batch syntheses. Parts a−d of Figure S2 (Supporting Information) show the decreasing residence times at a constant power of 300 W, while parts e and f show the effect of different power settings at a fixed residence time. The temperatures obtained are also indicated. At 300 W and at different residence times (Figure S2a−d, Supporting Information), the reaction temperature was constant at 90 °C. However, when the power was changed to 150 and 600 W, the temperature changed to 85 and 100 °C, respectively.

The effect of microwave power on the syntheses is shown in Figure S3 of the Supporting Information. K-OMS-2 nanoma-

terials synthesized at 150, 450, and 600 W at 10 mL/min and with 10% DMSO had impurity phases present. Only at 300 W was a pure phase obtained.

Finally, we studied the effect of reactor configuration on the syntheses. For this study, the coiled tubular reactor was replaced with a noncoiled one made from a similar material and with similar dimensions. Upon replacing the coiled reactor with a noncoiled one, the residence time changed significantly. For instance, at 10% DMSO and 10 mL/min flow rate, the residence time was only 1.5 min as compared to 4 min for the coiled reactor. This difference led to a phase that could largely be ascribed to γ-MnO$_2$. Figure S4 (Supporting Information) shows the results obtained. At a slightly slower rate of 5 mL/min, the phase started transforming to K-OMS-2 with a 3 min residence time.

The FTIR spectra of K-OMS-2 materials prepared under microwave continuous flow conditions are shown in Figure 5. The materials prepared exhibited the typical K-OMS-2 infrared spectra corresponding to Mn−O stretching modes[30a,b] in the region 800−400 cm^{-1}. Additional bands were observed in the region 1150−950 cm^{-1}. These bands appear at ∼1120, ∼1050, and ∼950 cm^{-1}. Another band is observed at 1633 cm^{-1}.

Morphology. Figure 6a shows the morphology of the MC-0-10 mL/min sample prepared in the absence of DMSO. The sample shows agglomerated nanospheres of diameters averaging about 200 nm. This is an amorphous phase, as can be confirmed by the XRD pattern. Figure 6b is for the sample MC-5-10 mL/min (5% DMSO). Both parts a and b of Figure 6 show similar features (agglomerated nanospheres), but unlike part a, part b shows isolated fibers and also the presence of a third phase of manganese oxide. Materials in Figure 6b unlike part a were synthesized in the presence of 10% DMSO and at a higher flow rate of 40 mL/min. With the flow rate set at 20 mL/min and % DMSO increased to 25%, a single pure phase of K-OMS-2 nanoparticles with fibrous morphology was obtained, as shown in Figure 6c. Increasing the % DMSO to 50% (MC-50-20 mL/min) and holding the flow rate at 20 mL/min, a similar fibrous morphology of K-OMS-2 nanoparticles was obtained. Synthesis of K-OMS-2 under conventional reflux yields materials with similar fibrous morphologies but longer fiber lengths, and is normally achieved after prolonged heating of 24 h. Figure 7 shows HRTEM images of the samples prepared at a flow rate of 20 mL/min and 25% DMSO (MC-25-20 mL/min). Figure 7a taken at a lower magnification reveals K-OMS-2 images with
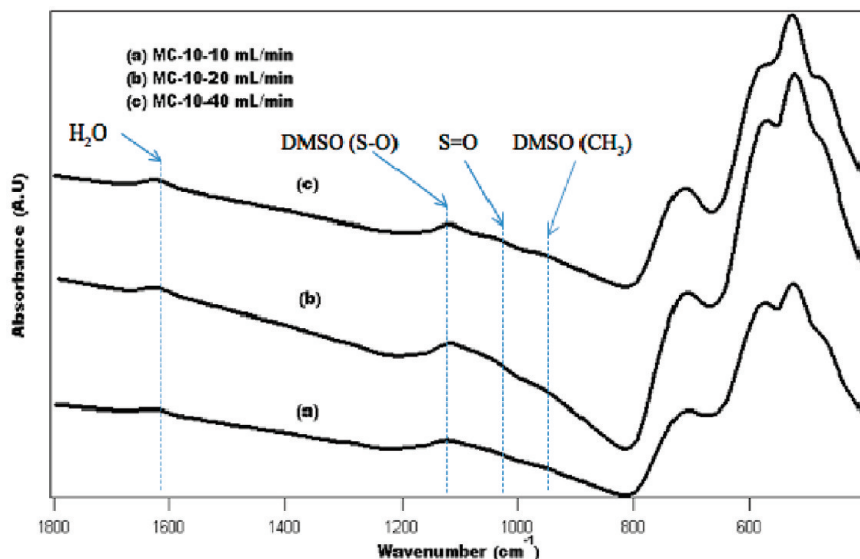
Synthesis of Manganese Oxide OMS-2 Nanomaterials

J. Phys. Chem. C, Vol. 114, No. 34, 2010 **14421**

Figure 5. FTIR spectra of OMS-2 materials: (a) MC-10-40 mL/min; (b) MC-10-20 mL/min; (c) MC-10-10 mL/min. Samples were synthesized at a microwave power of 300 W.
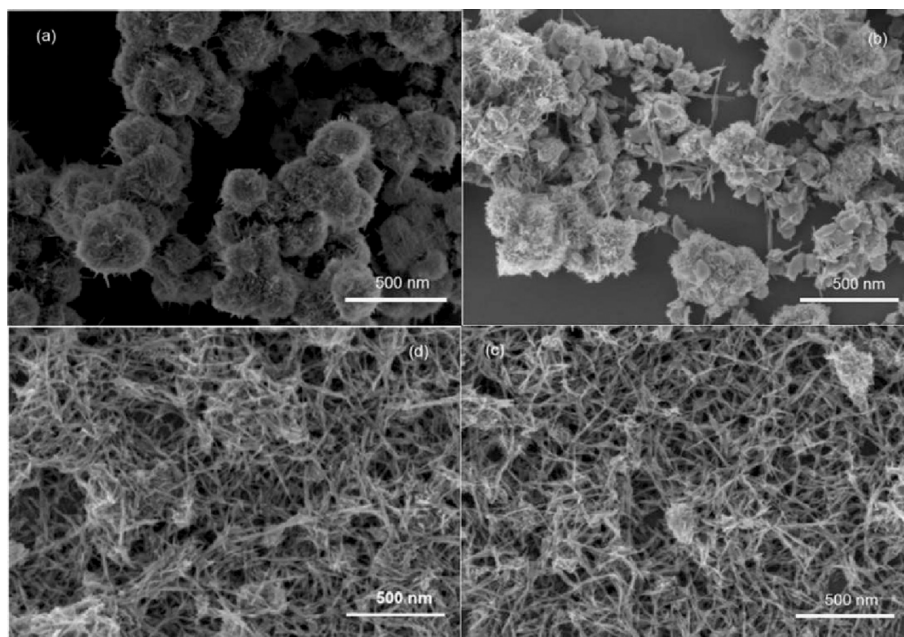

Figure 6. FESEM of K-OMS-2 materials (a) MC-0-10 mL/min (0% DMSO), (b) MC-10-40 mL/min (10% DMSO), (c) MC-25-20 mL/min (25% DMSO), and (d) MC-50-20 mL/min (50% DMSO). The scale is 500 nm.

much smaller K-OMS-2 nanofibers. The diameter of the smaller of the particles is about 5 nm, and fibers with lengths as small as about 20 nm can be observed. The HRTEM micrograph in Figure 7b reveals lattice fringes of 0.48 nm which can be indexed to the (200) lattice planes. It also indicates that the orientation of K-OMS-2 is aligned with the tunnel along the *c*-axis of the fibers.

Thermal Stability. TGA and DSC were used to study the thermal stability of the synthesized materials. Three samples were used for this study, as shown in Figures 8 and 9. These samples were MC-10-10 mL/min, MC-10-20 mL/min, and MC-50-20 mL/min. All of the samples showed similar TGA and DSC weight loss profiles with slight variations in the temperatures and weight losses. Three major TGA weight loss events occurred between 40−250, 350−600, and 650−820 °C at a ramp rate of 20 °C/min and in an inert (nitrogen) atmosphere. For MC-10-10 mL/min, the percent weight losses were 6, 7, and 1%, respectively, for the MC-10-20 mL/min, the weight

losses were 5, 9, and 1%, respectively, and for the MC-50-20 mL/min, the weight losses were 5, 8, and 2%, respectively. Almost similar TGA profiles have been reported and the species evolved probed using temperature programmed desorption (TPD) for K-OMS-2 materials synthesized conventionally without DMSO.[15,17h] The DSC profile showed four thermal events occurring for these materials with slight variations. These were endothermic peaks in the range 50−150 °C and exothermic peaks in the ranges 200−250, 280−320, and 340−380 °C.

Potentiometric Titrations. These titrations were performed on sample MC-25-20 mL/min giving a value of 3.9 as the AOS for manganese in this sample. This value is in agreement with AOS measurements from other reports.[15]

Surface Area. Table 1 shows the surface areas of the synthesized materials. The surface area ranges from 153 to 213 m^2/g, while the representative N_2 sorption isotherms are shown in Figure 10. Sample MC-5-10 mL/min was used to obtain representative nitrogen sorption data.
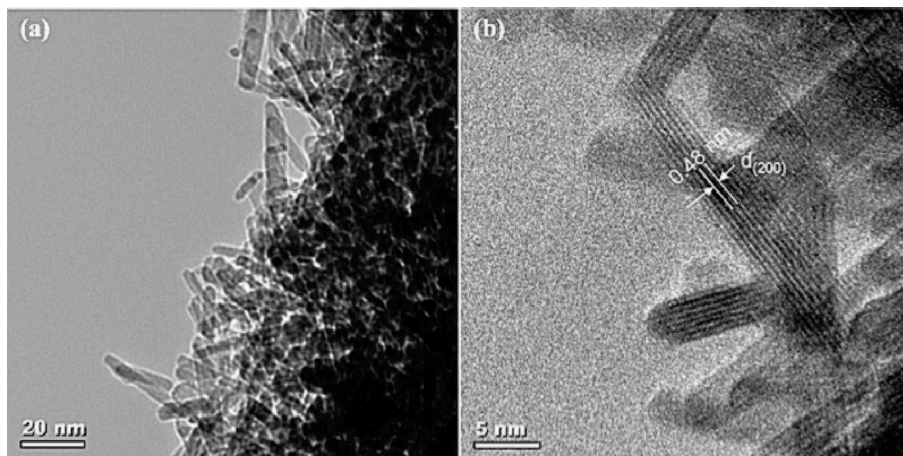
Figure 7. Low resolution (a) and high resolution (b) TEM images of K-OMS-2 materials prepared by the continuous flow microwave technique at 20 mL/min in 25% DMSO (MC-25-20 mL/min).
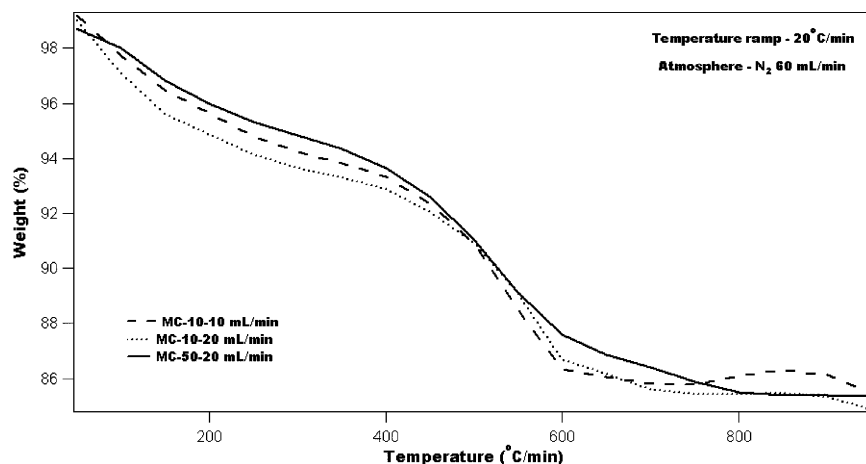

Figure 8. TGA profiles of K-OMS-2 materials prepared continuously at different flow rates (10 and 20 mL/min) with different volumes of DMSO (10 and 50%).
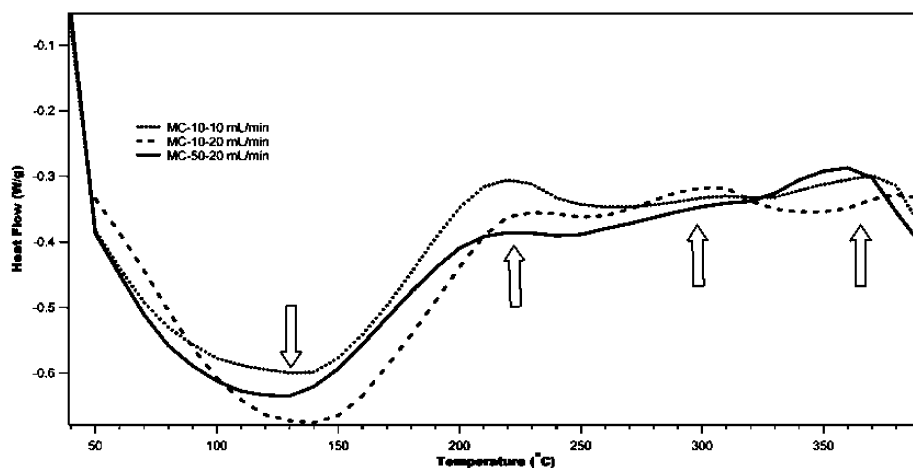

Figure 9. DSC profiles of K-OMS-2 materials prepared continuously at different flow rates (10 and 20 mL/min) with different volumes of DMSO (10 and 50%).

Catalytic Activity. We used the synthesized materials in the catalytic oxidation of 2,3,6-trimethylphenol in the presence of TBHP. The oxidation of TMP to 2,3,6-trimethyl benzoquinone (TMQ) is important due to its use as an intermediate in the synthesis of vitamin E. The synthesized nanomaterials showed excellent activity in the oxidation of TMP with 100% selectivity to the desired product. These results are tabulated in Table 2.

Discussion

Continuous Crystallization of K-OMS-2 Nanomaterials. In this report, the synthesis of K-OMS-2 was achieved using a continuous flow microwave technique. The crystallization of K-OMS-2 was obtained under specific conditions of reactant flow rate, volume of DMSO, and microwave power using a
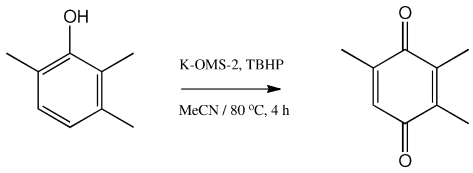
TABLE 1: BET Surface Areas (S_{BET}) of K-OMS-2 Materials Synthesized by the Microwave Continuous Method

sample	$S_{BET} \pm 1$ (m²/g)
MC-5-10 mL/min	176
MC-10-10 mL/min	153
MC-25-10 mL/min	189
MC-25-20 mL/min	191
MC-50-10 mL/min	213
MR-90-25% DMSO[a]	227
conventional reflux[b]	91
reflux (1% H_2O_2)[c]	62

[a] Reference 27. [b] Reference 17h. [c] Reference 15.

coiled Teflon reactor. The organic component of the solvent system is responsible for the rapid formation of the K-OMS-2, since in its absence the K-OMS-2 phase is not obtained. This can partly be due to the excellent coupling of microwaves with DMSO. When $KMnO_4$ solution was added to the $MnSO_4 \cdot H_2O$ solution containing HNO_3, the mixture turned light brown in color, darkening with the addition of more $KMnO_4$ solution due to formation of a precipitate. This further addition resulted in a dark brown mixture, which did not change in color significantly upon addition of DMSO. The dark brown precipitate is a precursor that transforms to K-OMS-2 during the synthesis. The symproportionation of Mn^{7+} and Mn^{2+} is responsible for the formation of ordered K-OMS-2. Portehault et al.[18a] showed using volumetric titrations that ~99% of $KMnO_4$ had already reacted with ~91% of $MnSO_4$ within a very short period of mixing the reactant solutions. At the start of the experiment, the $MnSO_4$ solution is lightly pink, almost clear. Drop-wise addition of $KMnO_4$ solution immediately leads to formation of a brown mixture. This is attributed to the oxidation of Mn^{2+} by the MnO_4^-. The reduction potentials of MnO_2/Mn^{2+} and MnO_4^-/Mn^{4+} in acidic environments are 1.23 and 1.68 V, respectively,[18,32] and thus support this premise. However, the final mixture was thin enough to enable it to flow in a coiled reactor without clogging the system like a thick precipitate would. A batch microwave system[27] earlier developed explored the types of nonaqueous cosolvents suitable for the synthesis of K-OMS-2.

TABLE 2: Oxidation of TMP to TMQ Using Continuously Synthesized K-OMS-2 Nanofibers

TMP		TMQ	
catalyst	conversion (%)	selectivity (%)	TON
blank	trace	−	−
MC-5-10 mL/min	58	82	8
	90[b]	100[b]	14
MC-10-5 mL/min	48	75	6
	100[b]	100[b]	16
MC-10-10 mL/min	47	73	5
	86[b]	100[b]	14
MC-10-20 mL/min	46	85	6
	83[b]	94[b]	13
MC-50-20 mL/min	40	66	4
	91[b]	96[b]	14

[a] Quantification was based on GC-MS peak areas. [b] Catalytic tests performed in the presence of 2 mmol of TBHP, corresponding reactions were carried out with 1 mmol of TBHP. Turnover number (TON) calculated by (moles of product ÷ moles of catalyst). Blank reaction was carried out in the absence of catalyst and with 2 mmol of TBHP. (−) were not determined due to trace amount of product.

In this report, DMSO was identified as a suitable candidate to use in the continuous flow process. In making this choice, we relied on tan δ values in Table 3 and the fact that a similar batch system utilized DMSO as a cosolvent, leading to the K-OMS-2 phase in as little as 10 min.[27] Solvents in Table 3 can be categorized into three classes, namely, high microwave absorbers (tan δ > 0.5), medium absorbers (0.1 ≤ tan δ ≥ 0.5) and poor absorbers (tan δ < 0.1).

Water as a standard of comparison has a tan δ value of 0.123 and so is a medium absorber of microwaves. Water has been used extensively as a medium for many microwave-assisted
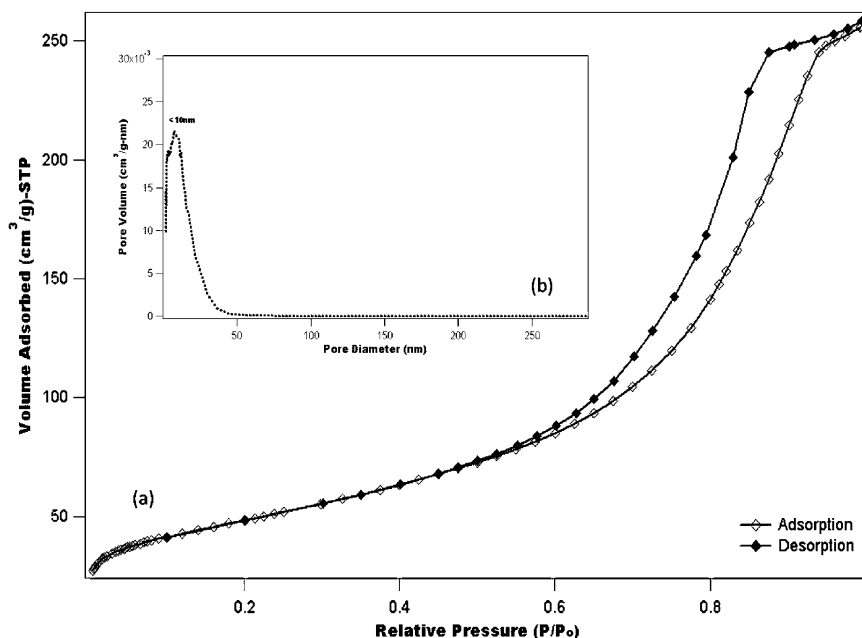

Figure 10. (a) Nitrogen sorption isotherm of the MC-5-10 mL/min K-OMS-2 sample and (b) the Barrett−Joyner−Halenda (BJH) pore size distribution.

14424 *J. Phys. Chem. C, Vol. 114, No. 34, 2010*

Opembe et al.

TABLE 3: Loss Tangents (tan δ) of Different Solvents (2.45 GHz, 20 °C)[10]

solvent	tan δ
ethylene glycol	1.350
ethanol	0.941
DMSO	0.825
2-propanol	0.799
formic acid	0.722
methanol	0.659
NMP	0.275
DMF	0.161
water	0.123
toluene	0.040
hexane	0.020

TABLE 4: Microwave Penetration Depth (2.45 GHz) in Selected Materials[34]

material	penetration depth (cm)	temperature (°C)
water	1.4	25
water	5.7	95
glass (borosilicate)	35	25
poly(vinyl chloride)	210	20
Teflon	9200	25
quartz glass	16000	25

syntheses. However, compounds above water in Table 3 are good absorbers of microwave radiation, resulting in superheating due to their high tan δ values. For instance, DMSO with tan δ = 0.825 is capable of being superheated.

The penetration depths of microwaves into reaction mixtures are usually limited, as shown in Table 4. Due to this, batch scale-up is usually limited in producing multikilogram quantities of material. This process was developed on the basis of the penetration depths of water, which are limited to 1.4 and 5.7 cm at 25 and 95 °C, respectively, as shown in Table 4. This means that for any meaningful scale-up in a reaction that utilizes water as a medium this limitation has to be overcome. Using a material that is almost transparent to microwaves and having a small diameter can overcome the penetration limitation of water. The Teflon coiled reactor (Φ_{inner} = 1/8") overcomes the depth limitation and enables microwaves to directly interact with the bulk of the reaction mixture. A coiled quartz reactor with similar dimensions may also be used, based on its penetration depth (see Table 4).

The effect of reactant flow rates that directly impacts the microwave residence time was investigated by comparing XRD patterns of samples prepared at different flow rates. At 40 mL/min, the reactant mixture resides for only 50 s in the microwave cavity. The XRD pattern for this sample reveals a poorly ordered manganese oxide phase (Figure 3). Transformation to a well-ordered crystalline K-OMS-2 phase occurs as the flow rate is slowed to 10 mL/min and even further slowed at 5 mL/min (Figure 3). Slower flow rates led to longer microwave residence times of 4 min at 10 mL/min and 8 min at 5 mL/min.

From the foregoing, transformation to crystalline K-OMS-2 occurs as the residence time is increased. With longer exposure times to microwaves, there is ample interaction time between the solvent and the microwaves, leading to better coupling and heating of the reactant materials. Cosolvent concentration also plays a crucial role in the transformation. When no DMSO is added to the synthesis mixture, transformation to K-OMS-2 does not take place. When mixed in water, DMSO with tan δ = 0.825 produces a solvent system capable of achieving superheating within a short time and is the reason the transformation to K-OMS-2 occurs even with a volume as low as 5%. Higher

concentrations of DMSO will lead to a better heating system, and a 50% DMSO system is expected to have an even better coupling and hence superheating. Materials prepared with any volume of DMSO from 5 to 50% led to XRD patterns that showed consistently broad peaks, an indication of the formation of small crystallites.

Microwave exposure time, power, and percent volume of DMSO act together to realize crystallization of K-OMS-2. At a faster flow rate of 20 mL/min, the reaction requires more DMSO of up to 25% to obtain a much purer phase of K-OMS-2 as compared to only about 10% at 10 mL/min. The shorter residence times contribute to shorter fiber lengths by restricting the crystal growth time and events that lead to lengthening of the fibers. The calculated crystallite sizes for the materials synthesized with various volumes of DMSO and at two different flow rates all show materials with average crystallite sizes in the 1.6−1.8 nm range. The exposure times under continuous flow conditions are believed to achieve a temperature not more than 100 °C.

In this report, small batch reactions were performed to study reaction temperatures. When the power is increased from 150 to 600 W, there is an increase in temperature from about 85 to 100 °C (see the Supporting Information). The temperature increases directly with power. Kinetically, the temperature increase has an effect on the reaction rate based on the Arrhenius equation (eq 1). At 100 °C, the rate is expected to be higher than that at 85 °C. As can be seen from Figure S3 of the Supporting Information, at 150 W, a poorly ordered manganese oxide phase is obtained which transforms to the correct phase at 300 W, while an increase to 450 and 600 W leads to impurity phases. The temperature measured by the thermocouple is the bulk temperature (T_b) and not the instantaneous temperature (T_i) resulting from the direct coupling of the microwave field and solvent's dipoles. Hayes et al.[38] use a similar approach. The instantaneous temperature should be much higher than the bulk temperature, hence leading to faster reaction rates. At 300 W, the optimal instantaneous temperature is realized to propel the reactant species to the transition state residing there for an optimal time period and then transforming to the correct phase. At 150 W, the instantaneous temperature is less than optimal and thus does not achieve this result, while at 450 and 600 W the heating is too rapid and propels the reacting species to the transition state too rapidly, leading to side and incomplete reactions resulting in impurities.

A coiled reactor led to synthesis of a pure K-OMS-2 phase. With a noncoiled reactor, reactant flow through the microwave cavity was too fast, since the coiling helped increase the residence time. A noncoiled reactor failed to lead to the formation of pure K-OMS-2 at the chosen flow rates. The samples that did not transform to the pure K-OMS-2 phase had an impurity phase that could be traced to γ-MnO_2.

Morphology and Crystal Structure. The synthesized samples showed a homogeneous fibrous morphology typical of cryptomelane-type K-OMS-2 materials. However, unlike K-OMS-2 materials synthesized conventionally, the morphology of these materials revealed much narrower fiber diameters. FESEM and HRTEM images of materials synthesized via this continuous flow route confirmed this feature. TEM shows the presence of nanofibers of varied lengths with lengths as small as about 20 nm and diameters of about 5 nm on average (Figure 7). Such ultrafine nanofibers contribute to the large surface area of these samples as compared to K-OMS-2 prepared under conventional reflux. The observation of lattice fringes also confirms the good crystallinity of this material.

Synthesis of Manganese Oxide OMS-2 Nanomaterials

J. Phys. Chem. C, Vol. 114, No. 34, 2010 **14425**

When no DMSO is added to the synthesis mixture, transformation to K-OMS-2 is hampered. FESEM of this material showed a largely amorphous phase of manganese oxide. Transformation to a well ordered K-OMS-2 and eventually to crystalline K-OMS-2 was tracked using X-ray diffraction, eventually forming K-OMS-2 with small fibers, as is evident in FESEM images (Figure 6).

Thermal Stability, Textural Properties, and Mixed Valency. Potentiometric titrations of the synthesized material reveal the existence of the mixed valent framework. The average oxidation state of 3.9 points to the existence of manganese in a mixture of oxidation states (+2, +3, and +4). The mixed valent nature of these materials has been studied before.[33] TGA and DSC results reveal that K-OMS-2 synthesized by the continuous flow technique compares well to the K-OMS-2 achieved via conventional means.[17h] The first TGA weight loss can be attributed to physically adsorbed water being desorbed from the surface of the material. The second weight loss can be attributed to evolution of chemically adsorbed water from the materials. The last weight loss can be assigned to evolution of structural oxygen from the materials. Carbon compounds from the presence of DMSO could also be evolved in these TGAs. The first peak of the DSC could be due to desorption of water from the materials and can possibly be linked to the first weight loss in the TGA profiles. The first exothermic peak starting at around 200 °C could be a result of physisorbed DMSO being driven off the materials. The last two events could be a result of decomposition of other compounds from the material, e.g., residual carbon compounds or species. The exact species evolved, and their evolution temperatures in this synthesis technique are subjects of further study using temperature programmed desorption (TPD) coupled with mass spectrometry (MS) techniques.

The Brunauer–Emmett–Teller (BET) surface areas of the samples are on average more than an order of magnitude (×2) higher than the average obtained for samples synthesized under conventional reflux techniques[15] and on average similar to K-OMS-2 synthesized via microwave reflux (batch) using a similar DMSO cosolvent system.[27] On the basis of IUPAC classification,[37] the representative sample MC-5-10 mL/min followed type II adsorption isotherms where a monolayer of N_2 molecules prevails at low relative pressures (P/P_o) and capillary condensation at high P/P_o. The sorption isotherms are similar to those obtained for materials synthesized through either conventional reflux[15] or microwave reflux.[29] The average BJH pore diameters are on average less than 10 nm.

FTIR spectra showed bands typical of K-OMS-2 and also revealed the presence of some extra bands. These bands can be attributed to the S–O stretch ($\sim$1120 cm^{-1}), the S=O stretch ($\sim$1050 cm^{-1}), and the DMSO–CH$_3$ rocking frequency ($\sim$950 cm^{-1}).[31] The K-OMS-2 tunnel water species[30b] can be observed at 1633 cm^{-1}. Nyutu[27] observed similar bands at higher DMSO levels. These bands could be attributed to residual DMSO on the surface of the synthesized samples. The presence of the DMSO bands on the solid samples indicates residual DMSO either physisorbed or chemisorbed. These data also suggest a secondary role played by DMSO, which could be a direct role in fiber growth processes.

Catalytic Activity. The synthesized materials performed exemplarily in the catalytic oxidation of TMP to TMQ. As shown in Table 2, all tested samples showed excellent conversions and selectivity to the desired product. The catalytic role of the material was confirmed by using a blank reaction (absence of catalyst) with 2 mmol of TBHP that resulted in trace amounts

of TMQ. With 1 mmol of TBHP, the conversions were lower than using twice as much TBHP. Samples with either 5% DMSO or 10% DMSO but synthesized at lower flow rates (5 and 10 mL/min) showed high activity (conversion of 100%) with concomitant high selectivity (100%) and turnover number of 16. By comparison, TMP oxidation is achieved using various compounds/catalysts. For instance, using copper(II) chloride in ionic liquids and 10 bar oxygen pressure yielded 98% TMQ.[35] TiO$_2$–SiO$_2$ aerogel using H$_2$O$_2$ as oxidant achieves a conversion of 94% with a TMQ yield of 89% after 1 h.[36] On the basis of the foregoing, the oxidation of TMP using the synthesized catalyst represents a milder and cheaper approach by comparison and still achieves similar results.

$$k = A \exp^{-E_a/RT} \tag{1}$$

Equation 1 shows the Arrhenius equation, where k is the rate constant, T is the absolute temperature, E_a is the activation energy, R is the gas constant, and A is the pre-exponential factor.

Conclusions

A continuous flow microwave technique has been developed for the synthesis of K-OMS-2 nanofibers. Process parameters such as flow rates, microwave power, volume of cosolvent (DMSO), and reactor type are crucial parameters for the final outcome. Slow flow rates (10 and 5 mL/min) led to crystallization of the K-OMS-2 phase with even lower volumes of DMSO (e.g., 5%). At higher flow rates (20 mL/min and higher), the crystallization of K-OMS-2 into a pure phase is also partly dependent on the amount of DMSO present. Lower volumes of DMSO at higher flow rates resulted in an impurity phase (γ-MnO$_2$). High microwave power levels (450 W and over) are not ideal; the optimal level for this synthesis is about 300 W. The synthesized materials performed well in the oxidation of TMP to TMQ, achieving high conversions (100%) and selectivity (100%). With this technique, the synthesis of K-OMS-2 on a multikilogram level is possible, since the only limitation to the synthesis is the size of the reagent reservoir. When a small reservoir is used, the reservoir replenishment rate is the limiting factor.

Supporting Information Available: A pictorial of the actual microwave setup used in the continuous flow synthesis and additional characterization. This material is available free of charge via the Internet at http://pubs.acs.org.

References and Notes

(1) Bohnemann, J.; Libanori, R.; Moreira, M. L.; Longo, E. *Chem. Eng. J.* **2009**, *155*, 905.

(2) Garringer, S. M.; Hesse, A. J.; Magers, J. R.; Pugh, K. R.; O'Reilly, S. A.; Wilson, A. M. *Organomet. Chem.* **2009**, *28*, 6841.

(3) Gharibeh, M.; Tompsett, G. A.; Conner, W. C.; Yngvesson, K. S. *ChemPhysChem* **2008**, *9*, 2580.

(4) Campbell, N. L.; Clowes, R.; Ritchie, L. K.; Cooper, A. I. *Chem. Mater.* **2009**, *21*, 204.

(5) Dandia, A.; Singh, R.; Khaturia, S.; Merienne, C.; Morgant, G.; Loupy, A. *Bioorg. Med. Chem.* **2006**, *14*, 2409.

(6) Baghurst, D. R.; Mingos, D. M. P. *Chem. Soc. Rev.* **1991**, *20*, 1.

(7) Gabriel, C.; Gabriel, S.; Grant, E. H.; Halstead, B. S.; Mingos, D. M. P. *Chem. Soc. Rev.* **1998**, *27*, 213.

(8) Tompsett, G. A.; Conner, W. C.; Yngvesson, K. S. *ChemPhysChem* **2006**, *7*, 296.

(9) Kappe, C. O. *Angew. Chem., Int. Ed.* **2004**, *43*, 6250.

(10) Hayes, B. L. *Microwave Synthesis: Chemistry at the Speed of Light*; CEM Publishing: Mathews, NC, 2002.

(11) Kingston, H. M.; Haswell, S. J. *Microwave-Enhanced Chemistry. Fundamentals, Sample Preparation and Applications*; American Chemical Society: Washington, DC, 1997.

(12) (a) Loupy, A. *Microwaves in Organic Synthesis*, 1st ed.; Wiley-VCH: Weinheim, Germany, 2002. (b) Lidström, P.; Tierney, J. P. *Microwave-Assisted Organic Synthesis*; Blackwell Publishing: Oxford, U.K., 2005. (c) Kappe, C. O.; Stadler, A. *Microwaves in Organic and Medicinal Chemistry*; Wiley-VCH: Weinheim, Germany, 2005. (d) Loupy, A. *Microwaves in Organic Synthesis*, 2nd ed.; Wiley-VCH: Weinheim, Germany, 2006. (e) Larhed, M.; Olofsson, K. *Microwave Methods in Organic Synthesis*; Springer: Berlin, 2006.

(13) (a) Kappe, C. O. *Angew. Chem., Int. Ed.* **2004**, *43*, 6250. (b) Hayes, B. L. *Aldrichimica Acta* **2004**, *37*, 66. (c) Nüchter, M.; Ondruschka, B.; Bonrath, W.; Gun, A. *Green Chem.* **2004**, *6*, 128. (d) Roberts, B. A.; Strauss, C. R. *Acc. Chem. Res.* **2005**, *38*, 653.

(14) Jas, G.; Kirschning, A. *Chem.—Eur. J.* **2003**, *9*, 5708.

(15) Villegas, J. C.; Garces, L. J.; Gomez, S.; Durand, J. P.; Suib, S. L. *Chem. Mater.* **2005**, *17*, 1910.

(16) (a) Post, J. E. *Proc. Natl. Acad. Sci. U.S.A.* **1999**, *96*, 3447. (b) Post, J. E.; Burnham, C. W. *Am. Mineral.* **1986**, *71*, 1178. (c) Feng, Q.; Kanoh, H.; Miyai, Y.; Ooi, K. *Chem. Mater.* **1995**, *7*, 148.

(17) (a) Son, Y. C.; Makwana, V. D.; Howell, A. R.; Suib, S. L. *Angew. Chem., Int. Ed.* **2001**, *40*, 4280. (b) Shen, Y. F.; Zerger, R. P.; DeGuzman, R. N.; Suib, S. L.; McCurdy, L.; Potter, D. I.; O'Young, C. L. *Science* **1993**, *260*, 511. (c) DeGuzman, R. N.; Shen, Y. F.; Neth, E. J.; Suib, S. L.; O'Young, C. L.; Levine, S.; Newman, J. M. *Chem. Mater.* **1994**, *6*, 815. (d) Chen, X.; Shen, Y. F.; Suib, S. L.; O'Young, C. L. *J. Catal.* **2001**, *197*, 292. (e) Xia, G.-G.; Tong, W.; Tolentino, E. N.; Duan, N.-G.; Brock, S. L.; Wang, J.-Y.; Suib, S. L.; Ressler, T. *Chem. Mater.* **2001**, *13*, 1585. (f) Shen, X. F.; Ding, Y. S.; Liu, J.; Laubernds, K.; Zerger, R. P.; Polverejan, M.; Son, Y. C.; Aindow, M.; Suib, S. L. *Chem. Mater.* **2004**, *16*, 5327. (g) Suib, S. L. *Annu. Rev. Mater. Sci.* **1996**, *26*, 135. (h) Ding, Y.-S.; Shen, X.-F.; Sithambaram, S.; Gomez, S.; Kumar, R.; Crisostomo, V. M. B.; Suib, S. L.; Aindow, M. *Chem. Mater.* **2005**, *17*, 5382. (i) Zhang, Q.; Luo, J.; Vileno, E.; Suib, S. L. *Chem. Mater.* **1997**, *9*, 2090. (j) Kim, S. H.; Kim, S. J.; Oh, S. M. *Chem. Mater.* **1999**, *11*, 557. (k) Ching, S.; Roark, J. L. *Chem. Mater.* **1997**, *9*, 750. (l) Jothiramalingam, R.; Viswanathan, B.; Varadarajan, T. K. *Catal. Commun.* **2005**, *6*, 41. (m) Feng, Q.; Kanoh, H.; Miyai, Y.; Ooi, K. *Chem. Mater.* **1995**, *7*, 148. (n) Sauvage, F.; Baudrin, E.; Tarascon, J.-M. *Sens. Actuators, B* **2007**, *120*, 638. (o) Kijima, N.; Takahashi, Y.; Akimoto, J.; Awaka, J. *J. Solid State Chem.* **2005**, *178*, 2741.

(18) (a) Portehault, D.; Cassaignon, S.; Baudrin, E.; Jolivet, J.-P. *Chem. Mater.* **2007**, *19*, 5410. (b) Garces, L. J.; Hincapie, B.; Makwana, V. D.; Laubernds, K.; Sacco, A.; Suib, S. L. *Microporous Mesosporous Mater.* **2003**, *63*, 11. (c) Liu, J.; Son, Y. C.; Cai, J.; Shen, X.; Suib, S. L.; Aindow, M. *Chem. Mater.* **2004**, *16*, 276.

(19) Opembe, N. N.; Son, Y.-C.; Sriskandakumar, T.; Suib, S. L. *ChemSusChem* **2008**, *1*, 182.

(20) Kumar, R.; Sithambaram, S.; Suib, S. L. *J. Catal.* **2009**, *262*, 304.

(21) Ghosh, R.; Son, Y.-C.; Makwana, V. D.; Suib, S. L. *J. Catal.* **2004**, *224*, 288.

(22) Kumar, R.; Garces, L. J.; Son, Y.-C.; Suib, S. L.; Malz, R. E. *J. Catal.* **2005**, *236*, 387.

(23) Sriskandakumar, T.; Opembe, N.; Chen, C.-H.; Morey, A.; King'ondu, C.; Suib, S. L. *J. Phys. Chem. A* **2009**, *113*, 1523.

(24) Jin, L.; Reutenauer, J.; Opembe, N.; Lai, M.; Martenak, D. J.; Han, S.; Suib, S. L. *ChemCatChem* **2009**, *1*, 441.

(25) O'Young, C. L.; Shen, Y. F.; Zerger, R. P.; Suib, S. L. Hydrothermal synthesis of octahedral molecular sieves, U.S. Patent 5,340,562, Aug 23, 1994.

(26) Yuan, J.; Laubernds, K.; Villegas, J.; Gomez, S.; Suib, S. L. *Adv. Mater.* **2004**, *16*, 1729.

(27) Nyutu, E. K.; Chen, C.-H.; Sithambaram, S.; Crisostomo, V. M. B.; Suib, S. L. *J. Phys. Chem. C* **2008**, *112*, 6786.

(28) Nyutu, E. K. Processing and optimization of functional ceramic coatings and inorganic nanomaterials. Ph.D Thesis, University of Connecticut, Storrs, CT, 2008.

(29) Crisostomo, V. M. B. New synthetic routes to catalytically active Manganite, K-OMS-2 and K-OMS-2/silicon dioxide and a preliminary study on the use of a continuous flow microwave technique in the synthesis of nanosized manganese and cerium oxides and cobalt and iron oxyhydroxides. Ph.D Thesis, University of Connecticut, Storrs, CT, 2008.

(30) (a) Potter, R. M.; Rossman, G. R. *Am. Mineral.* **1979**, *64*, 1199. (b) Gao, T.; Glerup, M.; Krumeich, F.; Nesper, R.; Fjellrag, H.; Norby, P. *J. Phys. Chem. C* **2008**, *112*, 13134.

(31) Elbaum, R.; Vega, S.; Hodes, G. *Chem. Mater.* **2001**, *13*, 2272.

(32) Antelman, M. S. *The Encyclopedia of Chemical Electrode Potentials*; Plenum Press: New York, 1982.

(33) Post, J. E.; Von Dreele, R. B.; Buseck, P. R. *Acta Crystallogr.* **1982**, *B38*, 1056.

(34) Bogdal, D. *Microwave-assisted organic synthesis. one hundred reaction procedures*; Elsevier: Oxford, U.K., 2005.

(35) Sun, H.; Harms, K.; Sundermeyer, J. *J. Am. Chem. Soc.* **2004**, *126*, 9550.

(36) Trukhan, N. N.; Kholdeeva, O. A. *Kinet. Catal.* **2003**, *44*, 347.

(37) Sing, K. S. W.; Everett, D. H.; Haul, R. A. W.; Moscou, L.; Pierotti, R. A.; Rouquerol, J.; Siemieniewska, T. *Pure Appl. Chem.* **1985**, *57*, 603.

(38) Hayes, B. L. *Aldrichchimica Acta* **2004**, *37*, 66.